AN EXPERIMENTAL INVESTIGATION ON NEAR-WALL PARTICLE SEGREGATION IN ENTRAINED-FLOW SLAGGING COAL GASIFIERS

Ramona Carbone*, Roberto Solimene*, Fabio Montagnaro, Maurizio Troiano***, Piero Salatino*****
solimene@irc.cnr.it; fabio.montagnaro@unina.it
*Istituto di Ricerche sulla Combustione, Consiglio Nazionale delle Ricerche, Piazzale Vincenzo Tecchio 80, 80125 Napoli (Italy)
**Dipartimento di Scienze Chimiche, Università degli Studi di Napoli Federico II, Complesso Universitario di Monte Sant'Angelo, 80126 Napoli (Italy)
*** Dipartimento di Ingegneria Chimica, dei Materiali e della Produzione Industriale, Università degli Studi di Napoli Federico II, P.le V. Tecchio 80, 80125 Napoli (Italy)

Abstract
This paper reports on preliminary results of an experimental investigation aimed at the development of a phenomenological model of the fate of coal/ash particles in entrained-flow slagging coal gasifiers, which considers the establishment of a particle segregated phase in the near-wall region of the gasifier. Mechanistic understanding of particle-wall interaction patterns has been carried out using the tool of the physical modeling. To this end, a cold flow model reactor has been designed and set up, where molten wax is air-atomized into a mainstream of air to simulate the fate of char/ash particles in a real hot environment. Sticky wall-sticky particle regime has been characterized, from a hydrodynamic point of view, by partitioning measurements between simulated segregated phases and by visual observation of the impact of sticky particles on the sticky wall.

1. Introduction
Modern entrained-flow coal gasifiers are characterized by operating conditions that promote ash migration/deposition onto the reactor walls, whence the molten ash is drained and quenched at the bottom of the gasifier as a vitrified slag [1-3]. The recent literature has addressed the fate of char particles as they impinge on the wall slag layer [3-5]. This research group has contributed [6-9] to develop a phenomenological model of the fate of coal/ash particles, which considers the establishment of a particle segregated phase in the near-wall region of the gasifier. This configuration can lead to an extensive coverage of the slag layer with carbon particles (segregation and coverage regime) beneficial to carbon conversion, as it gives rise to a longer mean residence time of carbon particles belonging to this segregated phase [6]. The phenomenological model has received some qualitative validation from analysis of the properties of ash streams generated in a full-scale entrained-flow gasification plant [7]. Moreover, the complex phenomenology

associated with interaction of a particle-laden turbulent flow with the inelastic slag-covered wall of the gasifier has been the subject of numerical simulations [8,9], that confirmed both a possible near-wall accumulation of particles and the relevance of such phenomenon on the performance of entrained-flow gasifiers. In the gasification chamber, coal particles are fed through nozzles as a lean-dispersed particle-laden gas flow. Inertial and turbophoretic mechanisms seem to be predominant, the first being enhanced by swirled or tangential flow, and the latter being active near the reactor walls. Moreover, inertia is relevant to coarser particles, turbophoresis to finer ones [6]. It is possible to classify all the possible particle-wall interaction patterns on the basis of the stickiness of both impinging particles and wall [5]:

i) Sticky Wall-Sticky Particle (SW-SP), in which char particles with high carbon conversion impinge on the slag layer (Fig. 1a);
ii) Sticky Wall-No Sticky Particle (SW-NSP), for particles with a low carbon conversion impinging on the slag layer [3,6] (Fig. 1b);
iii) No Sticky Wall-Sticky Particle (NSW-SP), when high carbon conversion char particles impinge on either dry wall or a carbon-covered ash layer (Fig. 1c);
iv) No Sticky Wall-No Sticky Particle (NSW-NSP), referring to low carbon conversion char particles impinging on either dry wall or a carbon-covered ash layer (Fig. 1d).

The particle or the wall is considered sticky when both the particle carbon conversion is above a certain critical (threshold) value (as explained by Li et al. [4], who set this value around 90%) and the temperature is above the ash melting point.

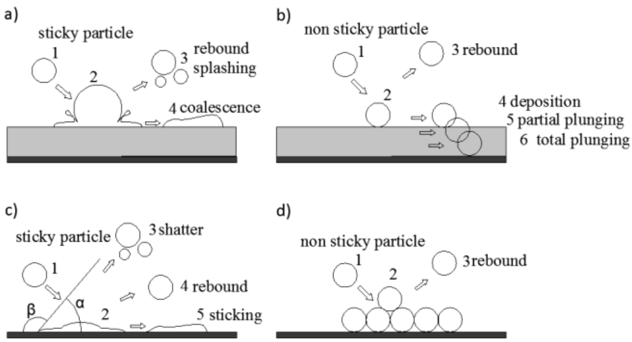

Figure 1. Micromechanical interaction patterns: a) SW-SP; b) SW-NSP; c) NSW-SP; d) NSW-NSP. (1) pre-impact, (2) impact, (3-6) post-impact.

This study aims at investigating near-wall particle segregation by using a lab-scale cold entrained-flow reactor. The cold flow model reactor ensures the formation of a dispersed phase and a near-wall layer to reproduce and characterize the four micromechanical interaction patterns depicted in Fig. 1. The present work, in particular, is focused on the study of the first regime (SW-SP) for which, after the droplets impact on the liquid layer, it is possible to have rebound and/or coalescence of droplets, as shown in Fig. 1a.

2. Cold flow model reactor and experimental features

Industrial entrained-flow slagging gasifiers operate at 'hard' conditions in terms of pressure and temperature, thus, a lab-scale cold flow model reactor has been designed, built-up and developed in order to permit the optical accessibility of the reactor walls. The plastic/fluid behaviour of softened or molten ash and of the wall slag layer has been simulated, at nearly ambient conditions, by molten wax as a surrogate of fuel ash. In this respect, the use of melted wax (1-hexadecanol) has been reported by Shimizu et al. [10], even if for a different application. After a screening of different candidates, Waradur E™ (Völpker, Germany) was selected, as the rheological/mechanical properties of this wax resembled those of a typical coal slag. Wax viscosity lies in the range 0.02-0.1 kg $m^{-1}s^{-1}$ as the temperature ranges between 130°C and 90°C, and wax density is around 1000 kg m^{-3}. Accordingly, the kinematic viscosity is in the order of 10^{-5}-10^{-4} m^2 s^{-1}, consistent with values reported in the literature for coal slag [2,3]. The kinematic viscosities of the wax are consistent with the establishment of laminar flow of the molten phase along the reactor walls. Besides, taking into account the surface tension (0.03 kg s^{-2} at 100°C), wax properties are such that the entrapment and over-layering criteria are not satisfied, and the segregation or segregation-coverage regime are likely to be established, as expected for realistic particle-slag interaction in entrained-flow gasifiers [6,7]. The wax was liquified and stored in a 9 L heated vessel. A three-way valve could be opened to convey the wax to the atomization vessel, consisting of air distribution and atomizer positioning sections. The atomization system generated a spray of molten wax in the model reactor which gave rise, upon deposition onto the wall, to a layer of molten wax. The nozzle was a commercial Delavan™ atomizer (AL model), designed so as to generate a spray of conical shape with an aperture angle of θ_{max}=25° and a uniform cross-sectional distribution of the atomized dispersed phase. Air-assisted atomization of wax resulted into droplets of 50-100 μm size. The reactor consisted of a Pyrex™ tube (D=0.04 m-ID). A mainstream of air was fed at the top of the air section, while the atomization air was fed directly to the nozzle. The schematic representation of the experimental apparatus and the parameters of the nozzle jet are reported in Fig. 2.

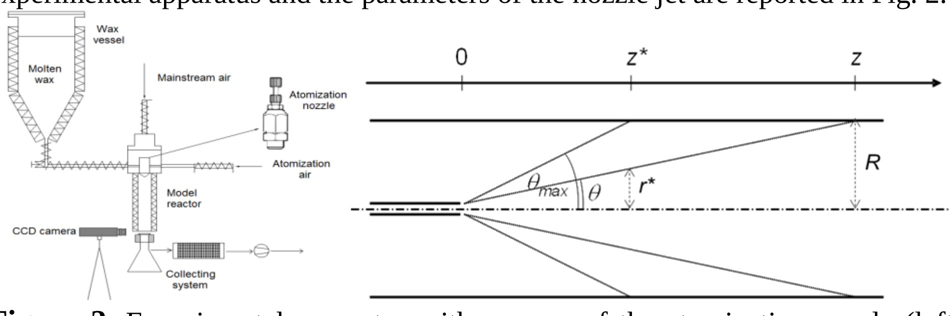

Figure 2. Experimental apparatus with a zoom of the atomization nozzle (left); geometrical parameters of the jet in the model reactor (right).

The operating conditions have been set on the basis of the ratio between the reactor volume and the fuel inlet mass flow rate commonly found for industrial gasifiers. This ratio is around 5 m^3 s kg^{-1}. Assuming as lab-scale model reactor a cylindrical tube of 0.04 m-ID and 1 m high, the fuel inlet mass flow rate is around 0.3 g s^{-1}. The inlet wax and air mass flow rates are 0.2 g s^{-1} and 1 m^3 h^{-1} (Q_a=0.3 m^3 h^{-1} for atomization air and Q_{ms}=0.7 m^3 h^{-1} for main air stream, both measured at 298 K), respectively.
In order to correctly operate the lab-scale reactor, three different temperatures have to be taken in account: the atomization temperature (T_a), i.e. the nozzle exit temperature, the main stream temperature, the wall temperature. The first one has to be set in such a way to ensure the complete liquid state of the wax droplets at the Pyrex tube inlet. Different aggregation states and viscosity values of wax in the dispersed phase can be reached by varying the main stream temperature. The wall temperature can be varied to assure the desired aggregation state and viscosity value of the wax wall layer. Thus, by tuning these three temperatures, it is possible to obtain the different micromechanical interaction patterns above discussed.
Experimental tests aimed at characterizing the phenomenology of the interaction between the dispersed phase generated by the spray and the reactor walls. For the SW-SP regime, partitioning measurements of the atomized wax between the dispersed and the wall phases were quantitatively assessed as a function of the distance from the nozzle. To accomplish this task, the reactor was equipped with a system (consisting by a vacuum flask, a trap, a filter and a pump) for the two phases wax collection at the bottom of the Pyrex tube. The mass flow rates in the dispersed phase and in the wall layer phase were obtained by dividing the amounts of wax cumulatively collected by the duration of the test. Visual observation and recording of the impact of sticky particles on the sticky wall was also accomplished by means of a CCD camera (Pulnix™ 6710) equipped with a magnifying zoom lens. The experiments were characterized by varying the main stream air flow rate and the Pyrex tube length.

3. Results and discussion

Partitioning measurements: Figure 3 reports the dilute-dispersed phase fraction of wax (y^{lean}) measured at the exhaust as a function of the reactor length (L) and of the main stream air flow rate. Figure 3a) reports values of y^{lean} measured in experiments carried out with different L-values, at fixed Q_a, Q_{ms} and T_a (0.3 m^3 h^{-1}, 0.7 m^3 h^{-1} and 145°C, respectively). It shows that y^{lean} abruptly decreases from nearly 0.91 in the proximity of the nozzle (L=0.03 m) to approach 0.12 for $L\geq0.20$ m. Figure 3a) also compares the experimental plot with limiting lines corresponding to idealized NSW-NSP and SW-SP regimes. In the first case (NSW-NSP), the wall reflects impinging particles according to a nearly elastic interaction pattern. Accordingly, y^{lean} would be 1 for any L. The other idealized limiting curve (SW-SP) is obtained by considering the conical shape of the jet and the uniform distribution of the dispersed phase across the jet (Fig. 2). Additional assumptions are that droplets impinging the wall under the effect of inertia are deposited thereon without rebound.

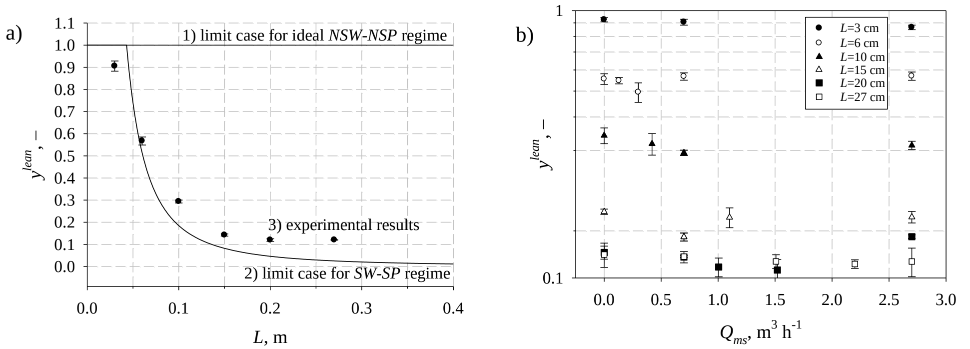

Figure 3. Effect of the tube length (a) and of the main stream gas flow rate (b) on the wax lean phase fraction.

According to the geometry of the nozzle and of the reactor (Fig. 2), the impact of molten wax droplets becomes significant only at a distance $z \geq z^*$ from the nozzle, the value of z^* being 0.043 m in the present case. Geometrical arguments suggest that:

$$y^{lean}(z) = \begin{cases} 1 & for \quad z < z^* \\ \dfrac{q\pi (r^*)^2}{q\pi R^2} = \left(\dfrac{r^*}{R}\right)^2 = \left(\dfrac{z^*}{z}\right)^2 & for \quad z \geq z^* \end{cases} \tag{1}$$

where q is the axial wax mass flux at $z=z^*$, and r^* and R are represented in Fig. 2. Equation (1) is plotted in Fig. 3a) as the idealized limiting curve corresponding to the SW-SP regime. Comparing the experimental data points with the limiting curves, the following features may be recognized: i) experimental data points lie much closer to the SW-SP regime limiting curve than to the other one, consistently with the operating conditions of the tests which promoted a molten status of both entrained wax droplets and of the wall layer; ii) values of y^{lean} slightly depart from 1 already at $z<z^*$. This behaviour is related to moderate backmixing of the dispersed phase associated with recirculation and main stream gas entrainment developing close to the nozzle; iii) the experimental data points lie somewhat above the theoretical SW-SP regime limiting curve for large values of L. This might result from either moderate droplet rebound at the wall followed by re-entrainment, or by a certain degree of ineffectiveness of inertial forces in promoting impingement and entrapment of droplets as they are simultaneously invested by the main stream flow directed parallel to the wall. It must be underlined that the transfer of droplets to the wall in the fully-developed flow downstream of the nozzle by Brownian or turbophoretic mechanisms is bound to be rather ineffective considering that the Reynolds number is in the order of 500.

Figure 3b) shows the effect of the main stream gas flow rate on y^{lean}: when L was fixed and varying Q_{ms} up to 2.7 m^3 h^{-1} at fixed T_a and Q_a (145°C and 0.3 m^3 h^{-1}, respectively), y^{lean} did not significantly vary. On the other hand, y^{lean} decreased as L increased at fixed Q_{ms}, in line with what observed in Fig. 3a). These findings further suggest that the axial profile of y^{lean} is largely dominated by the hydrodynamics of the jet.

Visual observations: Figure 4 reports two temporal sequences of snapshots captured by the CCD camera during a typical test (Q_a=0.3 m^3 h^{-1}, T_a=138°C and L=0.20 m). As a result of the impact of sticky particles on the sticky wall, coalescence was by far the predominant process, though occasional droplet rebound and re-entrainment into the dispersed phase could be observed.

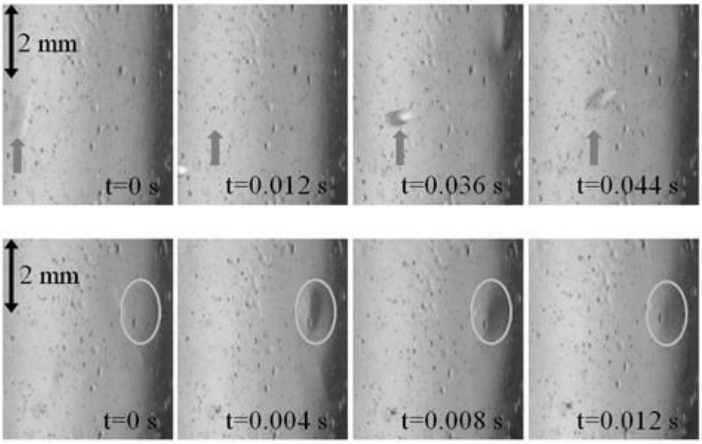

Figure 4. Rebound (up) and coalescence (down) of sticky wax droplets impinging on the sticky wax wall. Snapshots captured at a frame rate of 250 fps.

References

[1] Shimizu, T., Tominaga, H., *Fuel* 85:170–178 (2006).

[2] Ni, J., Yu, G., Guo, Q., Zhou, Z., Wang, F., *Energy Fuels* 25:1004–1009 (2011).

[3] Shannon, G.N., Rozelle, P.L., Pisupati, S.V., Sridhar, S., *Fuel Process. Technol.* 89:1379–1385 (2008).

[4] Li, S., Wu, Y., Whitty, K.J., *Energy Fuels* 24:1868–1876 (2010).

[5] Yong, S.Z., Ghoniem, A., *Fuel* 97:457–466 (2012).

[6] Montagnaro, F., Salatino, P., *Combust. Flame* 157:874–883 (2010).

[7] Montagnaro, F., Brachi, P., Salatino, P., *Energy Fuels* 25:3671–3677 (2011).

[8] Ambrosino, F., Aprovitola, A., Brachi, P., Marra, F.S., Montagnaro, F., Salatino, P., *Combust. Sci. Technol.* 184:871–887 (2012).

[9] Ambrosino, F., Aprovitola, A., Brachi, P., Marra, F.S., Montagnaro, F., Salatino, P., *Fuel* http://dx.doi.org/10.1016/j.fuel.2013.03.040 (2013).

[10] Shimizu, T., Haga, D., Mikami, G., Takahashi, T., Horinouchi, K., *Proc. 13th Int. Conf. Fluidization*, Gyeong-ju, Korea, Paper #83 (2010).